

Resilience Assessment of Urban Power Grid Under Extreme Disasters

Wenxin Guo
 College of Electrical Engineering
 Sichuan University
 Chengdu, China
 3438559272@qq.com

Chuan He
 College of Electrical Engineering
 Sichuan University
 Chengdu, China
 he_chuan@scu.edu.cn

Zihan Dong
 College of Electrical Engineering
 Sichuan University
 Chengdu, China
 2378375126@qq.com

Yitong Ning
 College of Electrical Engineering
 Sichuan University
 Chengdu, China
 201264715@qq.com

Abstract—In order to quantify the resilience of urban power grid to cope with extreme disasters, this paper proposes a multi-dimensional resilience evaluation system of power grid based on the consideration of disaster process performance and maximum risk prediction, taking into account the important load supply and social influencing factors of the city. In this paper, typhoon is taken as the representative of extreme disasters, and the typhoon wind field model and component fault model are established to realize the prediction of power grid damage probability. The Monte Carlo method is further used to simulate the fault situation of power system during typhoon. Then, through the power flow analysis, the resilience evaluation indices including the system performance drop speed, performance drop amplitude, average load loss, the lower bound of load loss, system load loss frequency and expected loss load time are calculated. Finally, the IEEE 33-bus system is established based on MATLAB simulation platform for case analysis. The results show that the proposed method can correctly and effectively evaluate the resilience of urban power grid under extreme weather, and provide reference for the extreme survival of urban power grid under extreme weather.

Keywords—extreme weather conditions, damage prediction, resilience assessment, Monte Carlo simulation, power flow, optimal dispatch

I. INTRODUCTION

The concept of resilience was first proposed by ecologist Holling in 1973 to measure the ability of ecosystems to absorb changes and disturbances and maintain stability [1]. With climate change and global warming, extreme natural disasters are becoming more and more frequent, which seriously threatens the normal and stable operation of the power system. And electricity plays an important role in the whole national economy. How to improve the stability of urban electricity consumption and ensure the supply of essential urban loads is particularly important. Therefore, scholars at home and abroad put forward the concept of “power grid resilience”, which is applied to the field of power system to study the resistance and recovery ability of power grid after serious disturbance. It is generally believed that the resilience system should include robustness, sensitivity, resilience, adaptability and other characteristics [2].

At present, the research on power system resilience assessment is mainly carried out from three parts. The first is to

analyze the law of power grid equipment failure caused by extreme disasters. Literature [3] proposes a novel risk assessment system for power towers under typhoon disaster, which is composed of data layer, knowledge extraction layer and visualization layer, based on equipment operation information, meteorological information and geographic information. Literature [4] employs a cascading failure evolution model considering short and long-time scales to analyze the cascading failures that may occur under extreme disasters. Literature [5] uses the cumulative distribution function of logarithmic normal distribution to fit the vulnerability curve parameters of various wire materials and wind attack angles with the finite element regression analysis method. The second is to construct a quantitative index of grid resilience. Literature [6] considers the ratio of restoration speed to length of disturbance and the area of the comparison area on the system performance curve under fault conditions and normal conditions to estimate resilience. In view of the severities of extreme weather events, the worst-case scenarios and the probabilistic failures of hardened components, literature [7] proposes a resilience evaluation index considering the weight of important loads. Literature [8] extends the “resilience triangle” model to the “resilience trapezoid” model, which is applied to the quantification of grid resilience, and proposes a grid resilience evaluation framework including four dimensions with quantitative indicators given for all four dimensions. The third is to improve the resilience assessment method. Based on the mechanism analysis and data-driven component failure model, literature [9] uses Monte Carlo simulation to generate the system state. For the system state with failure components, considering the inherent characteristics and interdependence characteristics of each system, a comprehensive energy flow is established to determine the minimum joint load shedding. Literature [10] dynamically studies the multi-component faults caused by disasters using the correlation function of transmission branch fault probability and typhoon wind speed, and proposes two methods based on time-varying Markov chain and dynamic Bayesian network to evaluate the ability of the system to resist extreme gusts.

Based on the above research, this paper carries out the parametric feature models considering the specific parameters of extreme weather, and uses the artificial intelligence algorithm to solve the failure probability of power grid components. Aiming at the operation of urban power grid under extreme

weather conditions, an optimal dispatching system for system resilience evaluation of urban power grid is established according to the state of power grid system under disaster disturbance.

II. PREDICTING THE PROBABILITY OF GRID DAMAGE

Due to the characteristics of low probability and high impact of extreme disasters, the characteristic parameters of extreme disasters are modeled, and the power grid component model is constructed to predict the failure of power system under natural disasters. At the same time, considering the disaster process performance and maximum risk prediction, in account of the important load supply and social influencing factors of the city, the resilience evaluation indices of the urban power grid are constructed.

A. Establishment of Parametric Typhoon Characteristic Model

In order to obtain the wind speed around the typhoon and predict the typhoon path, a typhoon wind field model is constructed. According to the typhoon-related information released by the meteorological department, the maximum wind speed radius can be obtained as follow:

$$\ln R_{max} = 2.636 - \mu \Delta p^2 + \eta \psi + \varepsilon \quad (1)$$

where $\mu = 0.00005086$; $\eta = 0.03949$; $\Delta p = 1013 - p_c$, p_c is the typhoon center pressure; ψ is the dimension value of the current typhoon center; ε is the correction coefficient whose value is 0~0.4, this paper takes 0.2.

Further, the typhoon gradient wind field at any point on the surface can be obtained from the distance to the typhoon center by computing.

$$V(x) = \begin{cases} \xi [1 - \exp(-\psi x)], & 0 \leq x < R_{max} \\ v_m \exp\left[-\frac{\ln \beta(x - R_{max})}{R_7 - R_{max}}\right], & R_{max} \leq x \leq R_7 \\ 0, & x > R_7 \end{cases} \quad (2)$$

$$\xi = K \times v_m, K > 1 \quad (3)$$

$$\psi = \frac{1}{R_{max}} \ln\left(\frac{K}{K-1}\right), K > 1 \quad (4)$$

where $V(x)$ is the wind speed of a certain point on the surface; v_m is the maximum wind speed measured at 10 meters above the ground; R_7 is the radius of the seven-stage wind circle; taking $K = 1.14$, $\beta = 10$ as the modeling factors for the specified typhoon boundary.

B. Establishment of Component Failure Probability Model Based on Parametric Typhoon Characteristic Model

1) Transmission line failure probability model

Overhead transmission lines are the most common equipment in power systems. They are easily affected by the surrounding environment because of the height and large span of the tower. Especially when the typhoon lands, overhead lines will bear a lot of wind pressure. If the stress limit exceeds the

mechanical strength of the equipment, it will cause irreversible damage.

Under the influence of typhoon weather, line faults are especially likely to be caused by wind damage. The external force that overhead transmission lines can withstand has its inherent limit. According to the theory of metal deformation, when the force of overhead lines exceeds its tolerance limit, its bearing capacity will decrease exponentially with the increase of strain, which will eventually lead to transmission line faults. In this paper, the following line fault probability model is established as follows:

$$P_{fv} = \begin{cases} 0, & 0 \leq v \leq V \\ \exp\left(\ln 2 \frac{v-V}{V}\right) - 1, & V < v_s \leq 2V \\ 1, & 2V < v_s \end{cases} \quad (5)$$

where P_{fv} is the fault probability of transmission lines under strong winds; v is the actual wind speed of the transmission line; V is the design value of the maximum wind speed of the transmission line. When $v \leq V$, the line outage probability is 0; When $v \geq 2V$, the line outage probability is 1; when $V < v < 2V$, the probability of line outage increases exponentially.

2) Tower failure probability model

According to historical statistics, the probability of line accidents directly broken by wires under typhoon disasters is low, and the main reason is tower failure instead. The failure rate is a local quantity index starting from the equipment level of the distribution network. However, Considering the disconnection fault caused by the collapse of the pole affected by the typhoon, it can reflect the real-time state of the equipment under the typhoon condition. The greater the failure rate of the line, the higher the vulnerability and risk value. The exponential curve function is used to fit the relationship between the failure rate γ_s of the pole s and the wind speed v_s at the position of the pole s as follows:

$$\gamma_s = \begin{cases} 0, & 0 \leq v_s \leq v_{min} \\ \exp[H(v_s - 2v_{min})], & v_{min} < v_s \leq 2v_{min} \\ 1, & 2v_{min} < v_s \end{cases} \quad (6)$$

where v_{min} is the maximum wind speed when the pole is designed; H is the model coefficient, and the value range is 0~0.4.

Since each line is equipped with several towers, according to the reliability evaluation theory of series system, the failure rate of line k can be obtained as follows:

$$F_k = 1 - \prod_{s=1}^{N_k} (1 - f_s) \quad (7)$$

$$f_s = 1 - e^{-\frac{\gamma_s}{1-\gamma_s}} \quad (8)$$

where N_k is the number of poles on the transmission line k ; f_s is the failure rate of pole s on the distribution line under typhoon weather.

III. SAMPLING METHOD BASED ON GRID DAMAGE

Because of the high uncertainty, wide influence range and serious consequences of extreme disasters, higher requirements are put forward for resilience assessment of power grid [11]. Therefore, a risk assessment method suitable for complex systems, non-sequential Monte Carlo method, is selected to evaluate the resilience of urban power grids under extreme disasters. The principle of the non-sequential Monte Carlo simulation method is to determine the state of the system components by random sampling the probability of the component state on the basis of the known component failure probability, and then combine the states of all components to obtain the system state.

Ignoring the interaction between component states, the state can be obtained as follows:

$$S_i = \begin{cases} 0, & R_i > Q_i \quad (\text{working state}) \\ 1, & 0 \leq R_i \leq Q_i \quad (\text{failure state}) \end{cases} \quad (9)$$

The state vector of a system consisting of N components is as follow:

$$\mathbf{s} = (s_1, \dots, s_i, \dots, s_N) \quad (10)$$

After a certain system state is selected for sampling, it can be judged whether it is invalid. If it fails, the risk index will be further calculated. When the number of samplings is large enough, the unbiased estimation of a state probability of the system is as follow:

$$P(s) = \frac{m(s)}{M} \quad (11)$$

where M is the total number of samplings; $m(s)$ is the number of times the system state s appears.

Furthermore, the system state frequency and the average duration of the system can be calculated according to the system state probability and transition rate:

$$f(s) = P(s) \sum_{k=1}^N \lambda_k \quad (12)$$

$$d(s) = 1 / \sum_{k=1}^N \lambda_k \quad (13)$$

where S_k denotes the transfer rate of the component k leaving state s , which includes the failure rate and the repair rate. Among them, the failure rate refers to the transition from the working state to the fault state, and the repair rate refers to the transition from the fault state to the working state.

IV. OPTIMAL DISPATCH UNDER EXTREME DISASTERS

The possible failure consequences of extreme disasters are generally serious and need to be analyzed in advance. When the transmission line is disconnected or the generator set is lost, if the power generation capacity of the remaining generator set is redistributed to meet the system load supply and line constraints, the load shedding amount of the system is 0. Otherwise the system fails, and part of the load must be reduced. The output of the remaining generator set is adjusted by power flow calculation, so that the load shedding in the fault state is as small

as possible. At this time, the line power flow of the system will be redistributed.

A. Objective Function

$$\min Z = \sum_j \sum_t \delta_{j,t}, j \in \Omega_J \quad (14)$$

where Z is the cutting load; Ω_J is the set of all nodes in the distribution network; $\delta_{j,t}$ is the active power of the load removed by the load d connected to the system node j at time t .

B. Constraint Conditions

1) Constraints of voltage and current of each node in the system

When the system is running, the voltage and current must be within a certain range as follow:

$$V_j^{\min} \leq V_{j,t} \leq V_j^{\max}, j \in \Omega_J \quad (15)$$

where $V_{j,t}$ is the voltage of node j at any time t ; V_j^{\max} and V_j^{\min} are respectively the lower and upper voltage limits of node j .

2) Constraints on the upper and lower limits of active and reactive power of each branch of the system

$$0 \leq P_{ij,t} \leq a_{ij,t} \cdot P_{ij,t}^{\max}, (i, j) \in \Omega_L \quad (16)$$

$$0 \leq Q_{ij,t} \leq a_{ij,t} \cdot Q_{ij,t}^{\max}, (i, j) \in \Omega_L \quad (17)$$

where $a_{ij,t}$ is the line state variable of the upper limit of active and reactive power flow.

3) Demand response constraints

When extreme disasters occur, the nodes participating in the load-side demand response can coordinate the load distribution of the system through load reduction and load transfer to reduce the load loss caused by disasters.

The demand response constraints are as shown in Formula (18)-(21). Formula (18) indicates that the predicted electrical load includes the node electrical load and the demand response electrical load after the demand response. Formula (19) expresses that the demand response electrical load is limited by the maximum load reduction and the maximum transferable load. As shown in the formula (20), the total demand response load within the running time range is not negative and cannot exceed the allowable load reduction limit. Formula (21) means that the reactive load of demand response is proportional to the active load.

$$P_{j,t}^{load} = P_{j,t}^{dr,LD} + P_{j,t}^{DR}, j \in \Omega_J \quad (18)$$

$$P_{j,t}^{load} - P_j^{load,max} \leq P_{j,t}^{DR} \leq a_j^{PDR} P_{j,t}^{load}, j \in \Omega_J \quad (19)$$

$$0 \leq \sum_t P_{j,t}^{DR} \leq P_j^{DR,max}, j \in \Omega_J \quad (20)$$

$$Q_{j,t}^{dr,LD} = Q_{j,t}^{load} / P_{j,t}^{load} \cdot P_{j,t}^{dr,LD}, j \in \Omega_J \quad (21)$$

where $P_{j,t}^{load}$, $Q_{j,t}^{load}$, $P_{j,t}^{dr,LD}$, $Q_{j,t}^{dr,LD}$ and $P_{j,t}^{DR}$ are respectively the predicted active power load, predicted reactive power load, active power load after demand response, reactive power load after demand response and demand response power load of

period t ; $P_j^{load,max}$ represents the maximum electrical load of nodes in the distribution network; α_j^{PDR} is the proportion of demand response electric load participation in period t ; $P_j^{DR,max}$ denotes the maximum load that can be reduced during the scheduling time.

4) Active and reactive power flow balance

The formula (22) is the active power flow balance formula, while the formula (23) is the reactive power flow balance formula.

$$\sum_{k \in s(j)} P_{jk,t} = P_{ij,t} - P_{j,t}^{dr,LD} + \delta_{j,t} + P_{j,t}^{DG} + P_t^{in}, j \in \Omega_j \quad (22)$$

$$\sum_{k \in s(j)} Q_{jk,t} = Q_{ij,t} - Q_{j,t}^{LD} + d_{j,t} \frac{Q_{j,t}^{LD}}{P_{j,t}^{LD}} + Q_{j,t}^{DG} + Q_t^{in}, j \in \Omega_j \quad (23)$$

where Ω_M is the set of lines; $s(j)$ represents the set of all child nodes with node j as the starting node; Ω_j is the set of all nodes in the distribution network; P_t^{in} is the active power transmitted from the superior power grid to the distribution network at time t ; Q_t^{in} is the reactive power transmitted from the superior power grid to the distribution network at time t ; $P_{ij,t}$ is the active power flow of the branch between system nodes i and j at time t ; $P_{j,t}^{DG}$ and $Q_{j,t}^{DG}$ are respectively the active power output and reactive power output of distributed generation at node j . The actual output of distributed generation cannot exceed a certain range, satisfying $P_{min} \leq P_{j,t}^{DG} \leq P_{max}$, $Q_{min} \leq Q_{j,t}^{DG} \leq Q_{max}$, where P_{min} , P_{max} are the maximum and minimum active power output of distributed generation, Q_{min} , Q_{max} are the maximum and minimum reactive power output of distributed generation; $P_{j,t}^{LD}$ is the active power consumed by the load connected to the system node j at time t ; $Q_{ij,t}$ is the reactive power flow of the branch between system nodes i and j at time t ; $Q_{j,t}^{LD}$ is the reactive power consumed by the load connected to the system node j at time t .

5) Node voltage drop, branch current and power relationship constraints

During the operation of the distribution network, the node voltage and branch current not only need to meet the size constraints, but also need to meet the constraints between each other or with the transmission power. The voltage of adjacent nodes is related to the transmission power on the branch and the branch impedance, while the current on the branch is related to the relationship between the node voltage and the transmission power of the line.

$$\begin{aligned} -(1-a_{ij,t})M &\leq -\frac{r_{ij} \cdot P_{ij,t} + x_{ij} \cdot Q_{ij,t}}{U_0} + U_{i,t} - U_{j,t} \\ &\leq (1-a_{ij,t})M, (i,j) \in \Omega_L \end{aligned} \quad (24)$$

where M is a sufficiently large number; r_{ij} , x_{ij} are respectively the resistance and reactance of the branch between system node i and j .

6) Loss of power load constraints

To ensure the safe, stable and economic operation of the power system, the power grid can remove the load of the removable part of the equipment if necessary. But its removable load size can not exceed the allowable range.

$$0 \leq \delta_{j,t} \leq P_{j,t}^{dr,LD}, j \in \Omega_J \quad (25)$$

V. SYSTEM RESILIENCE ASSESSMENT

The specific process of resilience assessment is as follows. Firstly, before the typhoon passes through, the meteorological information is obtained to speculate and predict the data, and the wind speed is estimated with the typhoon wind field model. According to the prediction results, the component failure probability model or artificial intelligence algorithm is used to solve the component damage probability. Then, according to the obtained component failure probability, the fault set is sampled by Monte Carlo simulation method, as the scene basis of the evolution of the power grid state. Afterwards, according to the system characteristics and fault scenarios, the stochastic power flow calculation is carried out to predict the system load loss and the output of the distributed power unit. Finally, according to the set resilience indices, the ability of the power grid to withstand disasters and return to normal is evaluated.

Extreme disasters are likely to lead to mass component failures in the power grid system, which will lead to large-scale blackouts and a sharp decline in system performance. In the process of disaster development, the system will enter the derating operation state. As the impact of extreme disasters decreases, the system will turn to the repair state and gradually return to the original normal operation state. The “toughness trapezoid” in the graph can be used to reflect the performance changes of the power system when it is affected by extreme disasters [12].

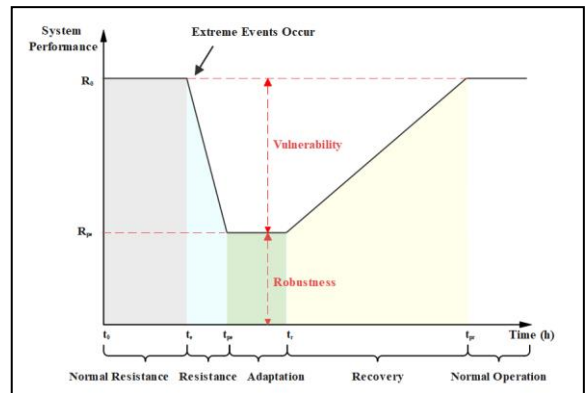


Fig. 1. System performance change curve.

According to the disaster development process, the power system state can be divided into four stages including pre-disaster prevention, disaster invasion, derating operation and post-disaster recovery.

The resilience level of the system during the whole fault evolution period is measured according to the system performance changes at different stages. And the performance drop speed (*PDS*) and performance drop amplitude (*PDA*) are calculated.

$$PDS = (R_0 - R_{pe}) / (t_{pe} - t_e) \quad (26)$$

$$PDA = R_0 - R_{pe} \quad (27)$$

where R_0 is the load level under normal operation of the system; R_{pe} is the minimum load level after the system encounters extreme weather invasion and derating operation; t_e is the initial time of the derating operation state of the system after extreme disasters; t_{pe} is the end time of disaster development.

In order to characterize the overall resilience level of the system under normal conditions, the average load loss (*ALL*) of the system is defined as the ratio of the minimum load loss of the system to the total number of simulations.

$$ALL = \sum_{n=1}^N \min Z / N \quad (28)$$

According to the example analysis, the infimum of the available system load loss (*ILL*) can reflect the resilience risk of the system, which is defined as the maximum value of the minimum load loss of the system in all cases.

$$ILL = \max(\min Z) \quad (29)$$

In the time range of the study, count the number of times that the system loses load due to insufficient power, and calculate the ratio of it to the total number of times as the system load loss frequency (*LLF*), which reflects the possibility of extreme disasters affecting the power system.

$$LLF = \frac{N_s}{N} \quad (30)$$

where N_s is the statistical number of load loss in the system.

Furthermore, the loss load expectation (*LLE*) in each given prediction time T can be obtained.

$$LLE = LLF \cdot T \quad (31)$$

VI. CASE STUDY

Because the energy attenuation is not large in a short time after typhoon landing, it is considered that the wind field model after landing is consistent with the landing point. The urban area is relatively small, so the moving path of the typhoon center can be regarded as a straight line, and the center moving speed is constant. This prediction principle is based on the idea of “extension”. And the typhoon moving path is predicted by using the constant moving speed and direction.

As a numerical calculation method based on random sampling, Monte Carlo simulation method simulates complex systems or problems by random sampling, using a large number of random sampling to approximate the solution of the problem, so as to obtain the numerical solution of the problem. Random numbers evenly distributed between (0,1) are randomly

generated and compared with the fault probability to obtain an array with a value of 0 or 1 to characterize whether the line is damaged. The accuracy is proportional to the number of samples. The larger the number of samples is, the closer the result is to the real situation. Under the condition that the fault probability is 0.3, the number of sampling is set to 1000 times. The damage of 32 lines is illustrated in the following figure.

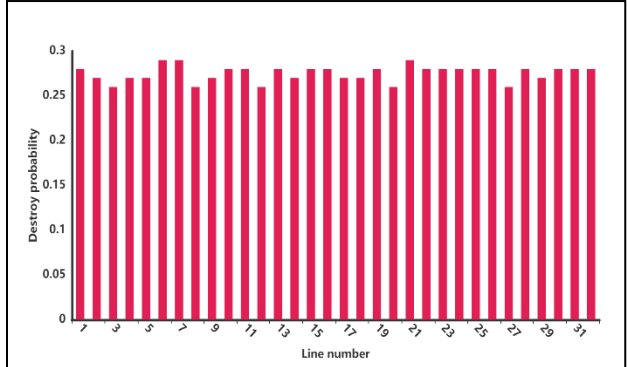


Fig. 2. Damage prediction of different lines.

Use the improved IEEE 33-bus system to verify the effectiveness of the proposed resilience assessment. On the MATLAB R2022 b platform, the Yalmip language is used to program and model, and the Gurobi optimizer is called to solve the minimum load loss model.

IEEE 33-node network is a typical low-voltage distribution network structure, which is widely used in power system science research. The improved IEEE 33-bus system includes a total of 1 substation, 2 distributed power units and 32 transmission lines, as shown in the figure. The distributed generation unit can be established according to the following methods: each row of the matrix corresponds to a node, each column of the matrix corresponds to a distributed generation unit. The row element corresponding to the node where the generator unit is located is 1, and the remaining row elements are 0. Based on the improved IEEE 33 node network, the power flow calculation power dispatch is used to obtain the active power output of each distributed power unit, as shown in the table.

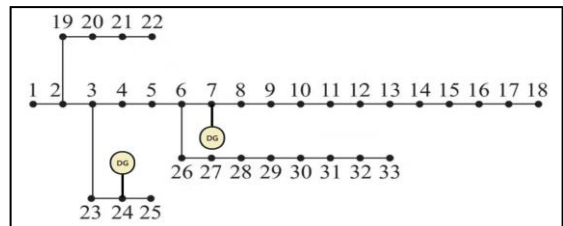


Fig. 3. Improved IEEE 33 node system.

TABLE I. ACTIVE POWER OUTPUT OF DISTRIBUTED GENERATION UNITS

Distributed Generation	1	2
Power Generation (MW)	0.3554	1.4946

By analyzing the active power and power loss load of 32 power load nodes at different times, it can be seen that the power load at 24 and 25 nodes is higher than that at other load points. The power loss load increases rapidly in a short time, and the outage risk is the largest. As shown in the following figure, the output of the distributed generation unit 2 is higher than 1 , because the vicinity of 2 is more affected by extreme disasters.

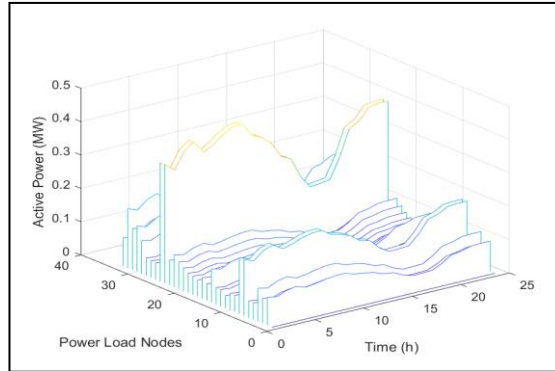


Fig. 4. Active power of power load nodes at different times.

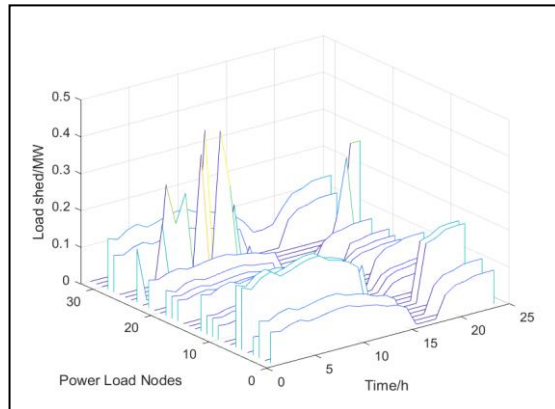


Fig. 5. Power loss load of the power load nodes at different times.

The load shedding data is collected and processed to obtain the resilience indices when the typhoon transit time is 34 hours. As shown in the following table, it can be seen that in the absence of reinforcement, maintenance and other measures, the system has a greater risk of failure when encountering extreme disasters.

TABLE II. SYSTEM RESILIENCE INDICES VALUE UNDER EXTREME DISASTERS

Resilience Assessment	Resilience Indices					
	PDS (MW/h)	PDA (MW)	ALL (MW)	ILL (MW)	LLF	LLE(h)
Value	97.288	32.105	30.996	95.011	0.846	29

According to the Monte Carlo sampling results, the failure probability of nodes 6,7,15,21,26 is relatively high, indicating a greater susceptibility to damage under extreme disasters. In the distribution network, the lines near the power supply play a decisive role in the operation of the system whose influence range are wider, so they are more important, such as between nodes 1 and 2, between nodes 6 and 7. Under normal circumstances, the transmission power among nodes 1~6 is significantly higher than that at other nodes, up to 60 MW. Besides, in the case of failure, the load loss at nodes 7,8,25 and 30 is large. Through comprehensive analysis of the probability of damage, the distance from the power supply, and the degree of load loss, it can be concluded that nodes 7 and 26 are important loads. Therefore, it is necessary to focus on improving their resilience to reduce the loss of the entire system.

REFERENCES

- [1] C. S. Holling, "Resilience and Stability of Ecological Systems".
- [2] National Infrastructure Advisory Council, "A framework for establishing critical infrastructure resilience goals," U.S. Department of Homeland Security (DHS), 2010.
- [3] H. Hou et al., "Risk Assessment and Its Visualization of Power Tower under Typhoon Disaster Based on Machine Learning Algorithms," *Energies*, vol. 12, no. 2, p. 205, Jan. 2019.
- [4] X. Zhang, W. Qin, X. Jing, J. Liu, X. Han, and P. Wang, "Power System Resilience Assessment Considering the Occurrence of Cascading Failures," in 2023 International Conference on Power System Technology (PowerCon), Jinan, China: IEEE, pp. 1–5, Sep. 2023.
- [5] L. Ma, P. Bocchini, and V. Christou, "Fragility models of electrical conductors in power transmission networks subjected to hurricanes," *Structural Safety*, vol. 82, p. 101890, Jan. 2020.
- [6] H. S. Dini, J. Jamani Jamian and E. Supriyanto, "Improving Resilience Index Quantification Using Weighted Sum Method," in 2023 IEEE Conference on Energy Conversion (CENCON), Kuching, Malaysia, pp. 103-107, Oct. 2023.
- [7] S. Ma, B. Chen, and Z. Wang, "Resilience Enhancement Strategy for Distribution Systems Under Extreme Weather Events," *IEEE Trans. Smart Grid*, vol. 9, no. 2, pp. 1442–1451, Mar. 2018.
- [8] M. Panteli, P. Mancarella, D. N. Trakas, E. Kyriakides, and N. D. Hatziargyriou, "Metrics and Quantification of Operational and Infrastructure Resilience in Power Systems," *IEEE Trans. Power Syst.*, vol. 32, no. 6, pp. 4732–4742, Nov. 2017.
- [9] H. Zhang, P. Wang, S. Yao, X. Liu, and T. Zhao, "Resilience Assessment of Interdependent Energy Systems Under Hurricanes," *IEEE Trans. Power Syst.*, vol. 35, no. 5, pp. 3682–3694, Sep. 2020.
- [10] E. Brugnetti, G. Coletta, F. De Caro, A. Vaccaro, and D. Villacci, "Enabling Methodologies for Predictive Power System Resilience Analysis in the Presence of Extreme Wind Gusts," *Energies*, vol. 13, no. 13, p. 3501, Jul. 2020.
- [11] R. Billinton and R. N. Allan, *Reliability assessment of large electric power systems*. in The Kluwer international series in engineering and computer science ; Power electronics and power systems, no. SECS 50. Boston: Kluwer Academic Publishers, 1988.
- [12] E. Hossain, S. Roy, N. Mohammad, N. Nawar, and D. R. Dipta, "Metrics and enhancement strategies for grid resilience and reliability during natural disasters," *Applied Energy*, vol. 290, p. 116709, May 2021.